IEEE Photonics Journal
An IEEE Photonics Society Publication

Open Access

Raman Spectroscopic Investigation of Sulfates Using Mosaic Grating Spatial Heterodyne Raman Spectrometer

Volume 11, Number 5, October 2019

Jun Qiu
Xiaotian Li
Xiangdong Qi

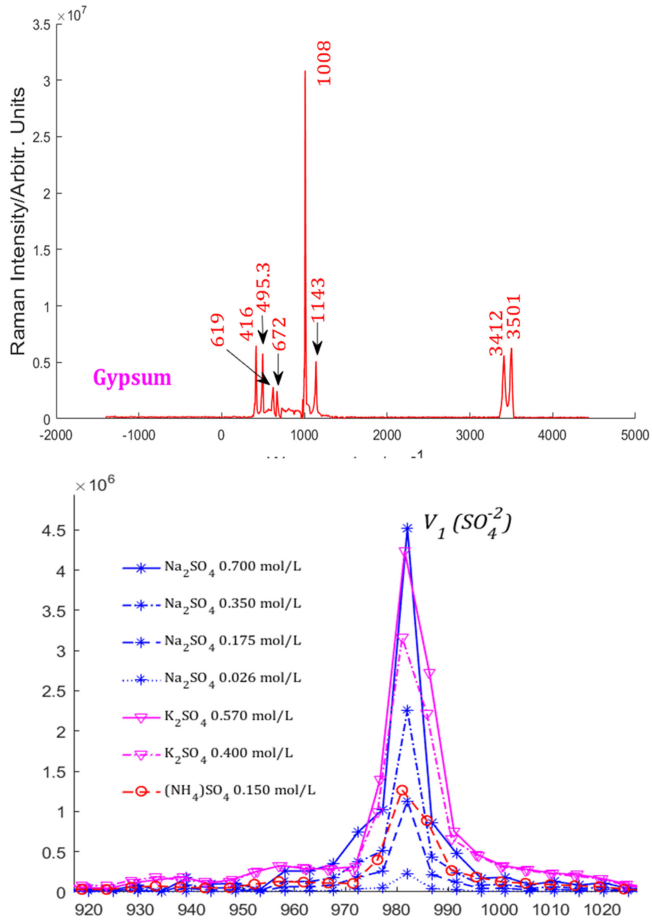

DOI: 10.1109/JPHOT.2019.2939222

Raman Spectroscopic Investigation of Sulfates Using Mosaic Grating Spatial Heterodyne Raman Spectrometer

Jun Qiu [1,2] **Xiaotian Li** [1] **and Xiangdong Qi**[1]

[1]Changchun Institute of Optics, Fine Mechanics and Physics, Chinese Academy of Sciences, Changchun 130033, China
[2]University of Chinese Academy of Sciences, Beijing 100049, China

DOI:10.1109/JPHOT.2019.2939222

Manuscript received June 8, 2019; revised August 22, 2019; accepted August 27, 2019. Date of publication September 3, 2019; date of current version September 19, 2019. This work was supported in part by the National Natural Science Foundation of China (NSFC) (61975255, 61505204), in part by Jilin Province Science and Technology Development Program Project in China (20190302047GX), and in part by Chinese Ministry of National Science and Technology (2014CB049500). Corresponding authors: Xiaotian Li and; Xiangdong Qi (e-mail: lixt_1981@163.com; chinagrating@263.net).

Abstract: We introduce a field-widened spatial heterodyne Raman spectrometer with a mosaic grating structure to investigate the broadband Raman spectra of sulfates. The broadband static spatial heterodyne Raman spectrometer configuration employs two mosaic gratings instead of the diffraction gratings to divide the broadband Raman spectrum into two bands. It is able to record high-resolution, broadband Raman spectrum range, covering 5740 cm^{-1} with 3.061 cm^{-1} spectral resolution using a regular CCD in a single-shot measurement. Raman spectra of mineral sulfates (celestine, gypsum) are investigated. This is the first time to conduct this Raman spectroscopic experiments to investigate the sulfates using the spatial heterodyne Raman spectroscopy. The sodium, potassium and ammonium sulfates at solid state and in aqueous solutions had been detected and analyzed. The effects of metal ions (K^+, Na^+, NH_4^+, Ca^{2+}, Sr^{2+}) on vibration of sulfate anion SO_4^{2-} were discussed. The main v_1 mode can be probed by the spatial heterodyne Raman spectroscopy to determine the concentration of sulfate and unambiguous identification of different sulfate minerals, solid sulfates.

Index Terms: Spectroscopy, spatial heterodyne spectrometer, broadband, high-resolution, field widening.

1. Introduction

A tiny portion of photons are scattered with a known wavelength and polarization after a sample is irradiated by a laser beam. In this process, the inelastic scattered photon is shifted to a different wavelength of the incident light, which either the energy (Stokes) is less than that of the incident photon or the energy (Anti-Stokes) higher than that of the incident photon. The phenomena of inelastic scattering light, which is known as the Raman effect [1]. Raman spectroscopy has been gaining popularity as a progressive method and technique for acquiring information about molecular vibrations due to requiring no sample preparation, providing significant cost saving, being non-destructive, and facilitating the direct analysis [2], [3].

Sulfates correspond to a large amount of salts, which are widespread in different forms and compositions in air, water and ground on Earth as well as Mars [4]. It has been reported that

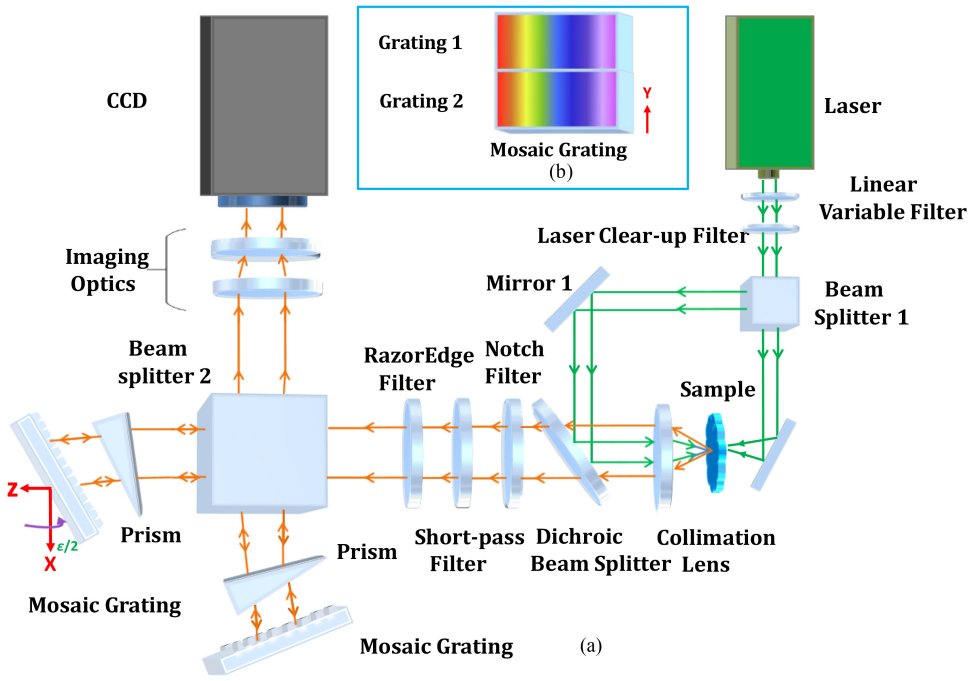

Fig. 1. (a) Schematic of Spatial heterodyne Raman spectrometer layout. (b) Definition of the mosaic grating.

the v_1 vibrational mode frequency of solid sulfates is dependent on the cations [4], [5]. A variety of sulfates is frequently presented as anhydrous or hydrated minerals, or dissolved in solution, such as sewage, industrial wastewater, pesticide residues, food additive, detergent and fertilizer. Raman spectroscopy has emerged as an effective tool for analyzing aqueous solutions because of the weak water Raman scattering effect. Recently, the investigations of cation effect on sulfate vibration modes have attracted increasing attention [4]–[8]. Numerous Raman studies have also been conducted for the detection and analysis of SO_4^{2-} in aqueous solutions [9], [10], which are essential for human health, industry, agriculture, and are very important to reveal the source of pollution in a water environment, as well as to study the origin of the chemical and physical transformations in geology.

Dispersive Raman spectroscopy and Fourier transform (FT) Raman spectroscopy are the two majors' technologies for collecting the Raman spectra. FT-Raman has advantages over dispersive Raman spectroscopy, such as higher optical throughput, high resolution, a superior frequency precision and spectral range. However, a traditional FT-Raman system has moving parts, and thus is relatively large in size and poor in terms of sensitivity and ruggedness. Recently, based on the Michelson interferometer modified for Raman by inclusion filters, the development of spatial heterodyne Raman spectroscopy (SHRS) has led to significant strides in Raman spectrometers, which combines robustness of a dispersive spectrometer with high spectral resolution and high throughput of an FT-Raman system.

SHRS is a novel Fourier transform (FT) spectrometer basing on the Michelson interferometer that two mirrors are replaced by gratings without any moving parts. Because of the primary advantages, such as high throughput, no moving parts and compact size, the SHRS is attractive as a static FT spectroscopy for Raman detections. However, in the SHRS system, there is an inverse relationship between the bandpass and spectral resolution, which makes it difficult to simultaneously satisfy the requirements of broadband pass and high spectral resolution. To solve the inherent problem of SHRS, a broadband and high-resolution static Mosaic Grating SHRS (MGSHRS) configuration based on the division of the required Raman spectrum range from low wavenumber to high wavenumber into multiplex narrow-bands is proposed. In Fig. 1, the proposed configuration uses

two mosaic gratings instead of the diffraction gratings to realize the requirements of high spectral resolution and broadband coverage.

Numerous Raman studies of sulfates have been reported [16]–[21]. In the Raman detections, spectra of sulfates were recorded using a dispersive Raman spectrometer or a FT spectrometer. However, the Raman spectrometers used in the previous work could hardly simultaneously satisfy the Raman requirements of high throughput, high resolution and broadband covering, in particular the Raman spectroscopy measurements of sulfates in water. In the typical SHRS system, there is the inverse relationship between the bandpass and spectral resolution. The MGSHRS breaks the limit and enables us to record broadband, high-resolution spectra with a regular CCD in a single-shot measurement.

In this present work, we are interested in the peak positions of sulfate bands, the influence of cation and the Raman OH stretching band of water (the OH stretch region at around 3000–3700 cm^{-1} in particular). In the MGSHRS system, a geometry for the interface of the laser to the target is designed to collect simultaneously both Raman backscattering and Raman transmission light. The properties of MGSHRS were calculated. This is the first time to use the MGSHRS to achieve the broadband and high resolution of the sulfates with a regular CCD in a single shot measurement. The Raman spectroscopy of sulfate minerals, solid sulfates and sulfates in aqueous solutions are presented. The results from investigations of cation effect on sulfate vibration modes at solid state and in aqueous solutions were discussed in details.

2. Experimental and Methods

2.1 Samples

Calcium sulphate dehydrate $CaSO_4 \cdot 2H_2O$ (gypsum) was chosen as mineral. The potassium, sodium and ammonium sulfates were purchased from Shanghai Macklin Biochemical Co., Ltd as the powdered forms, and the stated purity of the purchased samples was between 98% and 99%. The water was deionized. All the chemicals were used without further purification, cutting or polishing.

At the room temperature and atmospheric pressure, the different concentration ratios of aqueous solutions of sulfate were prepared. The volume of the deionized water per each tube was fixed to 10 mL. The concentration levels of selected potassium sulfates aqueous solution were 0.4 mol/L, and 0.57 mol/L. The sodium sulfate concentrations were 0.026 mol/L, 0.175 mol/L, 0.35 mol/L and 0.7 mol/L. The concentration level of the ammonium sulphate aqueous solution was 0.15 mol/L.

2.2 Instrumental

In Fig. 2, the main components of the instrument are commercially-available off-the-shelf, and can be separated into six logical groups: laser, Raman filters, Beamsplitter, two field widening prisms, two mosaic gratings, and detector. The ready availability of the continuous wave (CW) solid state laser power at 532 nm is linearly variable from 0 to 400 mW by the linear variable filter.

For instrumental simplicity and ease of use, the most commercial laser-based spectrometers were designed for observation in a backscatter arrangement. In the back-scattering Raman, geometry, the laser was focused at the surface of a sample, then the light emerged from the sample surface is collected. In the transmission Raman geometry, the laser beam was incident upon one side of the sample and the transmitted Raman light was collected from the opposite side. For more efficient collection of Raman signals from a sample, we had designed a novel geometry by adopting both the back-scattering collection geometry and the transmission collection geometry. In this collection geometry, the scattered radiation, including backscatter and transmission Raman, could be collected and collimated by the collimation lens. To remove the major problem associated with the Rayleigh line, the suitable 532-nm long pass filter (Semrock, LP03-532RU-25) and a 532-nm notch filter (Semrock, NF01-532U-25) were used to stop the Rayleigh scattered light. A 700-nm short-pass filter

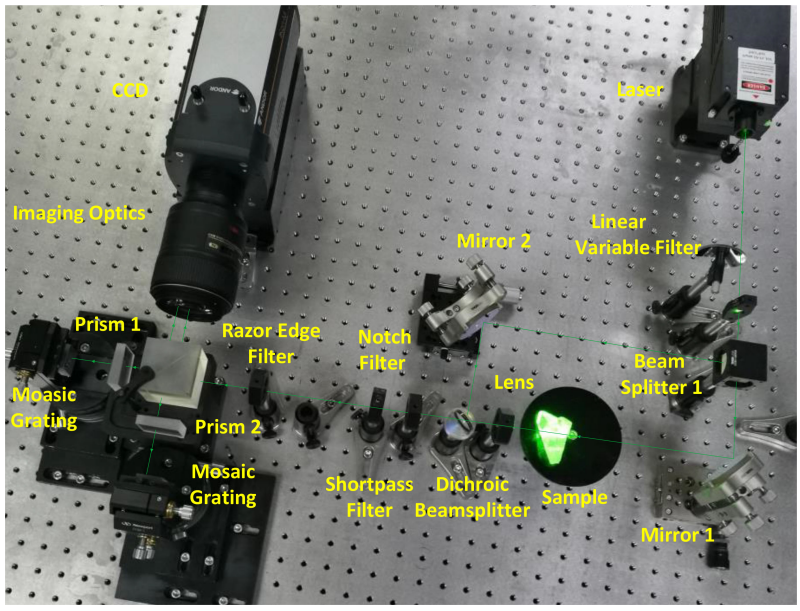

Fig. 2. Photograph of the actual schematic of Spatial heterodyne Raman spectrometer breadboard with a layout corresponding to Fig. 1.

(84-714, Edmund) was used to filter out the ambient light and fluorescent light at the wavelengths higher than 700 nm.

The filtered light is split into two by a 50.8 $\times$ 50.8 $\times$ 50.8 mm^3 cube beam splitter (model no. 20BC17MB.1, Newport). The bema splitter is used as an optical device and directs the beams of light onto the two field widening prisms and two mosaic gratings. The refractive index of two field widening prisms is 1.527, and the apex angle is 2.661°. One 150 grooves/mm diffraction gratings and one 130 grooves/mm diffraction gratings (Changchun Institute of Optics, Fine Mechanics and Physics, Chinese Academy of Sciences) form a mosaic grating. The mosaic gratings in MGSHRS are in Littrow configuration and are set to correspond to the Littrow wavelength. In our case, two mosaic gratings are operated at 1st diffraction order and one mosaic grating are rotated by a small angle $\varepsilon/2$ around x-axis to separate the overlapping wavenumber dependent. As the final spectrometer element, the CCD detector with 1024$\times$1024 pixels (iKon-M 934, Andor) is used to record the fringe image. The 2-dimensional (2-D) interferogram of SHRS can be written as [11]:

$$I(x, y) = \int_0^\infty B(\sigma)\{1 + \cos[2\pi(4(\sigma - \sigma_L)x \tan\theta_L + \sigma y\varepsilon)]\}d\sigma \quad (1)$$

where $B(\sigma)$ is the input spectral intensity as a function of wavenumber, σ is a wavenumber, σ_L is a Littrow wavenumber, and x is measured on the detector in the dispersion plane of the grating. The inverse Fourier transform of the interferogram yielded the transmission Raman spectrum.

The thermoelectrically cooled CCD detector operating at -60 °C to reduce the thermal noise within the sensor chip. Each sample is placed on front focal plane of the collimation lens, and the focal length of collimation lens is 25 mm. All the Raman measurements are carried out in full daylight by shielding the targets and instrument contact area using a black cloth under the room temperature. More detailed introductions about the basic theory of MGSHRS can be seen in Qiu *et al.* [12].

2.3 Calibration Methods

The calibration is needed in the initial instrumentation stage when a Raman interferometer is manufactured and tested. Generally, the wavelength calibration can be accomplished by using

calibration sources with known spectral lines like two lines an emission spectrum. This procedure established the spectral response of the instrument based on the spatial frequency response from the known input of the mercury lamp. We have used a mercury lamp for the purpose of wavelength calibration. Using the measured fringe cycles across the detector and the known wavelengths from the calibration source, the wavelengths corresponding to each spatial frequenies can be calculated [12]–[14].

The Raw fringe patterns are collected and stored as spe files using Andor SOLIS software. Because each pixel in the CCD detector sees a different interferometer path, the interferometer arms and MGSHRS detector are needed to be aligned with great attention. During the measurement, the gain and dark current of each pixel, the interferogram's center-burst shift from the zero-location on the detector and system vibration should be taken into consideration. Thus, for the conversion of the MGSHRS interferograms into calibrated spectra with real-time processing capability, the interferogram processing algorithm must be performed to deal with the realistic, interferometric data. Flat-fielding is the process of correcting the interferometric data for variations in the pixel-to-pixel sensitivity across the detector [15]. The phase correction method is used to correct the wavenumber-dependent phase error by implementing the FT shift theorem [16]. The wavelet threshold de-noising function is then used to effectively separate the signal from the noise. The Raman spectrum of sulphur is achieved by a commercial instrument (B&W Tek *i*-Raman pro) as calibrated Raman spectrum to correct the calibration error of Raman shift caused by the temperature shift of environment or movement of the instrument platform.

3. Results and Discussions

3.1 Properties of MGSHRS

The MGSHRS breadboard instrument performance parameters can be estimated by a calibration procedure. This procedure establishes the spectral response of the instrument based on the spatial frequency respond from the known input lines (576.964 nm, 579.588 nm) of a mercury lamp [12]–[14]. The Littrow wavelength equals to 535.587 nm. The Littrow angle, θ_L is given by:

$$\theta_L = arc\sin\left(\frac{\lambda_L \times G}{2}\right) \tag{2}$$

where G is the groove density, the Littrow angle is 2.283°.

Next, the spectral resolution δ_σ is inversely proportional to the Littrow angle and the width of the two mosaic gratings, as indicated by Eq. (3).

$$\delta_\sigma = \frac{1}{4W\sigma\sin\theta_L} \tag{3}$$

where the width of the two mosaic gratings that is imaged on the CCD camera equals 20.5 mm. So, the spectral resolution is calculated to be 3.061 cm^{-1}.

Last, a single bandpass can be expressed as:

$$\Delta\sigma = N\delta_\sigma \tag{4}$$

In our case, the two spectral ranges are not completely separated. And one spectral range is estimated to be -1521 cm^{-1} to 1613 cm^{-1}, the other spectral rang is estimated to be 1085 cm -1 to 4219 cm -1. Therefore, the total spectral range was extended to 5740 cm^{-1}.

3.2 Raman Spectra of Anhydrous Sulfate Minerals and Anhydrous Sulfates

Celestite is a sulfate mineral consisting strontium sulfate ($SrSO_4$), which is one of the most common sulfate minerals on earth. Currently, It is thought to be isostructural and belongs to a sulfate mineral with the barite structure [6]–[8]. In the crystal structure of celestine, the symmetry of the perfect tetrahedron is low, resulting in splitting of especially the v_3 and v_4 modes. According to the T_d symmetry of strontium sulfate, eleven Raman active modes theoretically exist in celestite

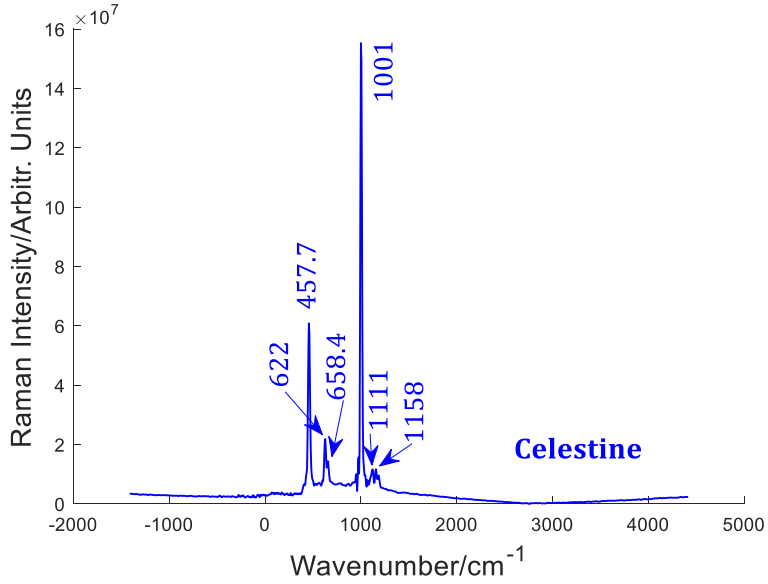

Fig. 3. The Raman spectrum of Celestine at the laser power of 45 mW with an integration time of 5 s.

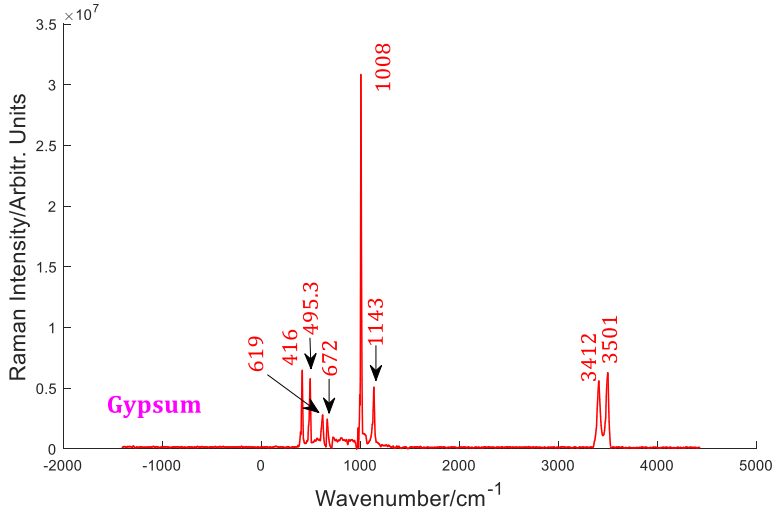

Fig. 4. The Raman spectrum of Gypsum ($CaSO_4 \cdot 2H_2O$) at the laser power of 60 mW with an integration time of 6 s.

at ambient pressure and room temperature [6]. However, six Raman bands could be detected in the Raman spectra of celestite, as shown in Fig. 3. The most intense v_1 band which corresponds to the symmetric stretching of SO_4^{2-} tetrahedra at 1001 cm^{-1}. The symmetric bending mode (v_2) appears at 622 cm^{-1}. The other characteristic bands, anti-symmetric stretching mode v_3 and symmetric stretching mode v_4 are both split into two bands.

Gypsum is the most abundant sulfate mineral in nature and widely used in construction or as fertilizer [8], [9]. Fig. 4 shows the spectra of gypsum both in the OH stretching region and free anion SO_4^{2-} region at room temperature. In high-shift region, the high Raman shifts are centered at 3412 cm^{-1}, and 3501 cm^{-1} as the v_1 symmetric stretch and v_3 asymmetric stretch modes of H_2O molecule, respectively. In low Raman-shift region, the v_2 mode is centered at 419 cm^{-1} and 495.3 cm^{-1}, the Raman peaks at 619 cm^{-1} and 672 cm^{-1} due to the v_4 mode, and the main peak

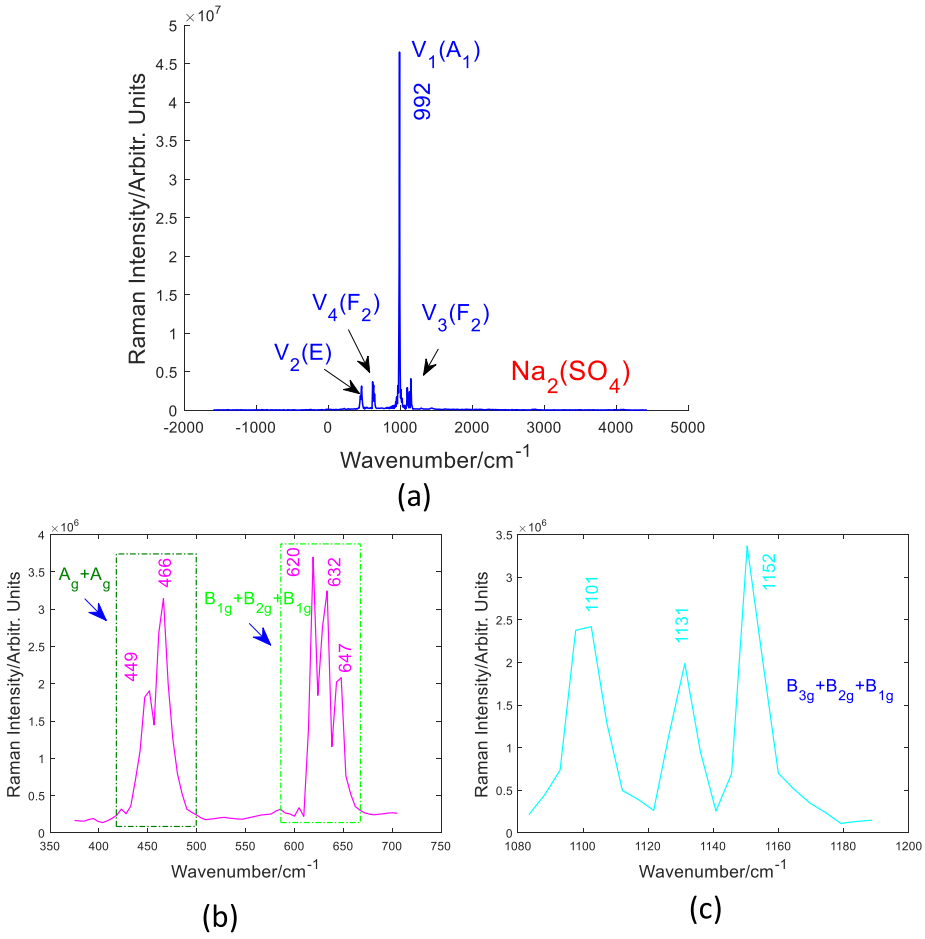

Fig. 5. The Raman spectrum of solid sodium sulfate (a), 380–710 cm^{-1} region showing v_2 and v_4 modes (b), and 1040–1200 cm^{-1} region including v_3 mode (c) at the laser power of 60 mW with an integration time of 8 s.

at 1008 cm^{-1} and 1143 cm^{-1} correspond to the v_1 symmetric stretch and v_3 asymmetric stretch modes of free anion SO_4^{2-}, respectively.

The Raman spectra of solid sodium sulfate (Na_2SO_4) is presented in Fig. 5. The most prominent feature of these spectra is the sulfate anion symmetric stretch (ν_1) at 992 cm^{-1}. The peak positions at 449 cm^{-1} and 466 cm^{-1} correspond to the symmetric bending v_2 mode, the Raman peaks at 619 cm^{-1} and 672 cm^{-1} due to the antisymmetric bending v_4 mode. The triplet v_3 modes of sodium sulfate appear at 1101 cm^{-1}, 1131 cm^{-1} and 1152 cm^{-1}.

Raman spectra recorded in solid sodium sulfate, potassium sulfate and ammonium are show in Fig. 5, Fig. 6 and Fig. 7, respectively. These three solid sulfates illustrate the same similarities, regardless of the nature of the cation. The most intense Raman peaks is clearly visible in the wavenumber range 975-992 cm^{-1}. The v_2 mode is occurs at about 449 cm^{-1}. The triplet v_3 mode appears between 1092-1152 cm^{-1}. The v_4 mode is lying in the 613-620 cm^{-1}. All the Raman shifts and assignments are expected to be in agreement with previous work [19]–[22].

Relationship between Raman band positions of SO_4^{2-} and ionic radii of cations are showed in Fig. 8. For the wavenumbers of Raman band positions of solid sodium sulfate, potassium sulfate and ammonium, datas show a remarkable decrease when passing from the solid sodium sulfate to the potassium sulfate, and then to the ammonium sulfate. Due to the polarizing power of cations which is defined as Z/r^2, where r is the radius and Z is the ion charge, so the wavenumber of Raman

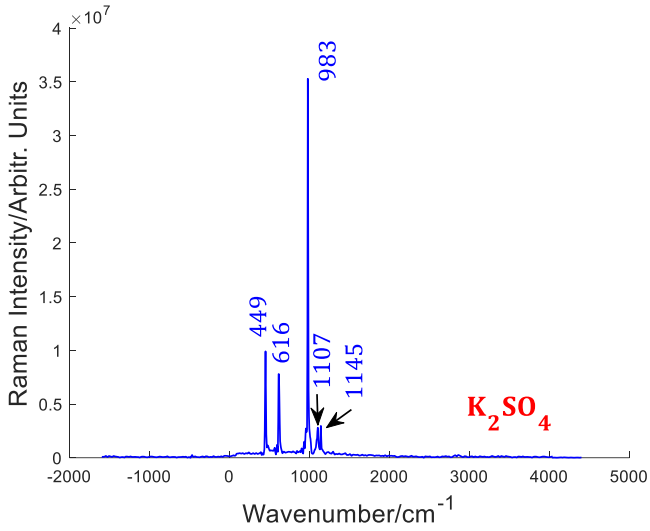

Fig. 6. The Raman spectrum of solid potassium sulfate (K_2SO_4) at the laser power of 60 mW with an integration time of 5 s.

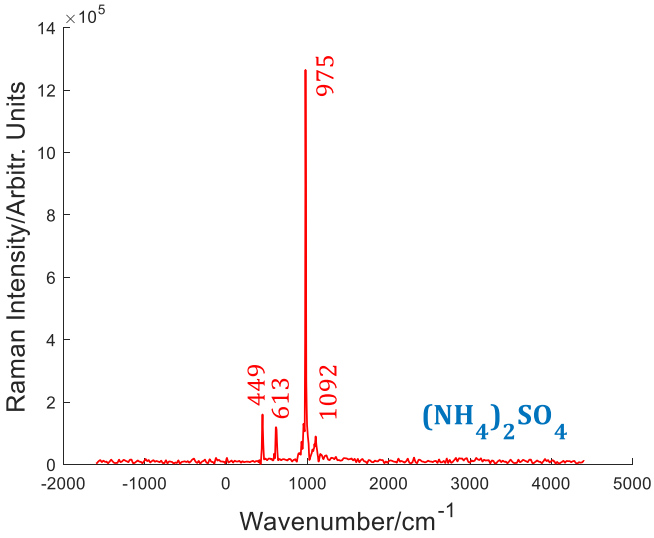

Fig. 7. The Raman spectrum of solid ammonium sulfate ($(NH_4)_2SO_4$) at the laser power of 80 mW with an integration time of 6 s.

band positions decreases as the polarizing power decreases [16]. But this effect is not observed in the Sr-rich and Ca- rich of sulfate minerals, which could be credited to the insufficient purity of these natural sulfate minerals.

3.3 Raman Analysis of Sulfates in Aqueous Solution

Compared to the Raman spectrum of solid sodium sulfate in Fig. 5 and the Raman spectrum of aqueous solution of sodium sulfate in Fig. 9, the Raman position of v_1 mode shifted to a low wavenumber region at 982 cm^{-1} [10]. The v_4 mode exhibits a similar shift to a low wavenumber region. The splitting of v_2, v_3 and v_4 vibration modes are clearly discernible. Moreover, the characteristic of OH vibration of water is obviously observed at an integrated region from 2800–3700 cm^{-1}. In Fig. 10, the v_1 (SO_4^{2-}) band shifts to a slightly low wavenumber. Meanwhile, the Raman spectrum of the potassium sulfate is broadened and downshift when going from the solid to solution. This is

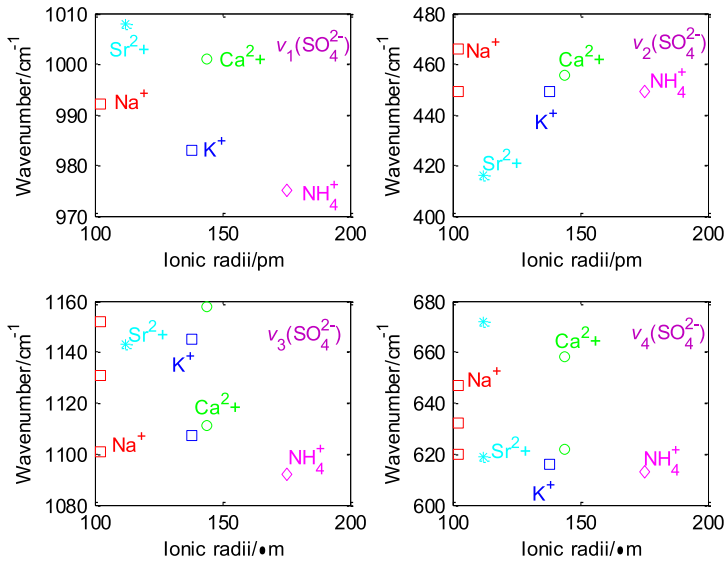

Fig. 8. Relationship between Raman band positions of SO_4^{2-} measured in solid sulfates and ionic radii of cations.

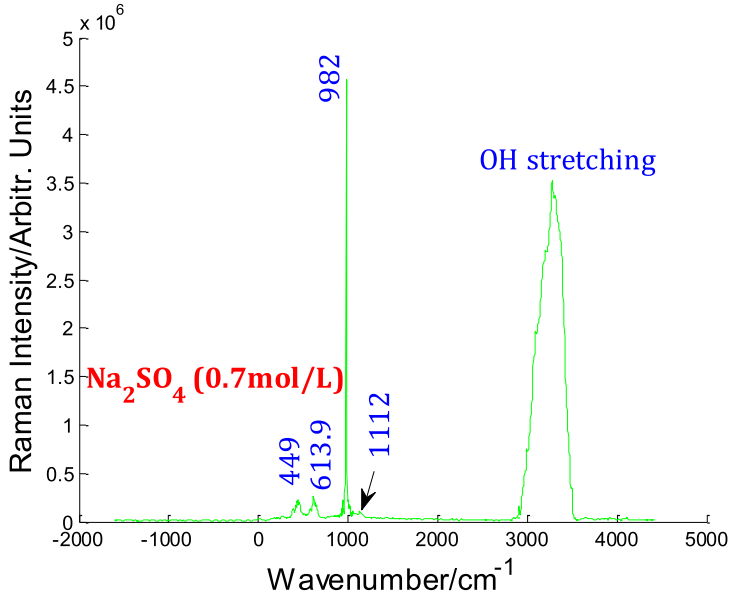

Fig. 9. The Raman spectrum of sodium sulfate (Na_2SO_4) in aqueous solution (0.7 mol/L) at the laser power of 108 mW with an integration time of 6 s.

because every atom of the SO4 molecule in solution vibrates freely, However, in the case of the solid sulfate, the atom vibrates under additional influences from the cations in crystal lattice, which caused the variation in the wave number of the absorption band [24].

A concentration profile of the v_1 (SO_4^{2-}) Raman bands of the aqueous sulfate salt solutions is presented in Fig. 11. Due to the symmetric profile of the v_1 (SO_4^{2-}) mode is independent of salt concentration and the strong the v_1 (SO_4^{2-}) mode in aqueous solutions, qualitative identification of the concentration can be achieved by the MGSHRS. The quantification needs two processes [18]: the intensity of the Raman signature peak is integrated over the whole wavenumber region 940 to 1020 cm^{-1} covered by the v_1 (SO_4^{2-}) mode, which includes the whole intensity under the peak, including the background; After the normalization and derived by the intensity of peak maximum in

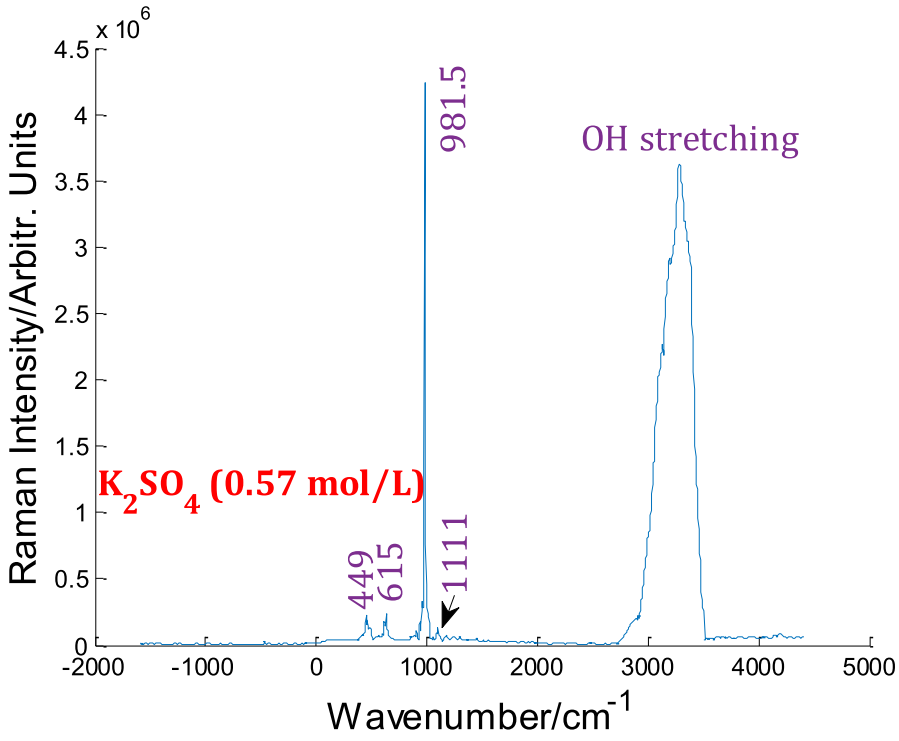

Fig. 10. The Raman spectrum of potassium sulfate (K_2SO_4) in aqueous solution (0.57 mol/L) at the laser power of 135 mW with an integration time of 6 s.

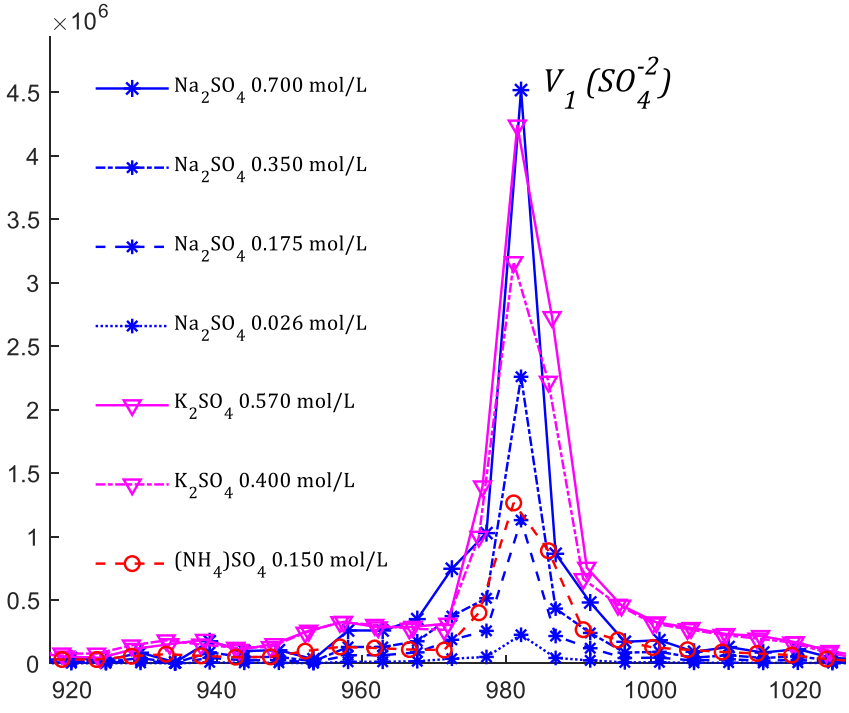

Fig. 11. The v_1 mode for sodium, potassium and ammonium sulfate aqueous solutions. The largest peaks of the three peaks correspond to the same weight content of salt in deionized water (10 mL), but to different molarities.

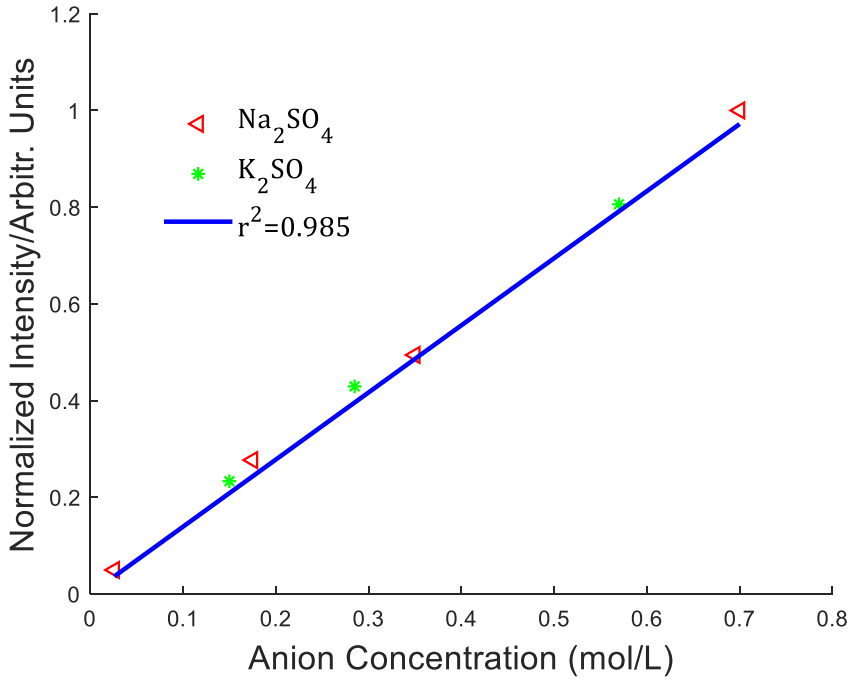

Fig. 12. Fitting curve of the sulfate in aqueous solution between peak area of the Raman line v_1 of SO_4^{2-} and the concentration in mol/L.

order to avoid a change due to any change external parameter in experimental conditions, such as the temperature, laser beam intensity.

In our case, the regression coefficient $r^2 = 0.985$ is obtained, proven to be an efficient and appropriate to determine the concentration of sodium sulfate (Na_2SO_4), potassium sulfate (K_2SO_4) and ammonium sulfate ($(NH_4)_2SO_4$) in water using our Raman spectrometer.

4. Conclusions

In this work, a breadboard for broadband and high-resolution Raman measurements has been designed and built. The proposed broadband static setup is based on using mosaic grating to create multiple narrow-band Raman spectra and combining the SHRS and mosaic gratings to operation of the spectrometer at a broadband spectral range with a high resolution in a single-shot measurement. We calculated the properties of MGSHRS, including the bandpass and spectral resolution. We have demonstrated for the first time that the MGSHRS has the ability to detect the mineral sulfates, solid sulfates and sulfates in aqueous solutions.

In the Raman spectra of solid sulfates were observed the four fundamental vibration modes of SO_4^{2-}, with variations in Raman band position and splitting, causing by the direct related to the size of metal cation radius. The metal cation dependence is not obvious and vanishes when the solid sulfate is dissolved in deionized water. It shows that the concentration of sulfate in aqueous solution could be achieved and determined after normalization and suitable calibration. The Raman spectrometer, which is accounted as a Raman sensor, could be used to determine concentration of sulfate or salt and unambiguous identification of different sulfate minerals, solid sulfate. We believe that the MGSHRS has a promising application in geochemistry, agriculture, environment and planetary science.

Author Contributions: J. Qiu proposed the idea and conducted the study. J. Qiu and X. Li designed and constructed the experimental setup. J. Qiu wrote the main manuscript text, prepared all the figures. J. Qiu and X. Li reviewed and revised the manuscript. X. Qi supervised the project.

References

[1] V. Raman and S. Krishnan, "A new type of secondary radiation," *Nature*, vol. 121, no. 3048, pp. 501–502, 1928.
[2] D. Li *et al.*, "Supra (carbon nanodots) with a strong visible to near-infrared absorption band and efficient photothermal conversion," *Light-Sci. Appl.*, vol. 5, no. 7, 2016, Art. no. e16120.
[3] X. Zhang *et al.*, "Optical visualization and polarized light absorption of the single-wall carbon nanotube to verify intrinsic thermal applications," *Light-Sci. Appl.*, vol. 4, no. 8, 2015, Art. no. e318.
[4] J. L. Bishop *et al.*, "Spectral identification of hydrated sulfates on Mars and comparison with acidic environments on Earth," *Int. J. Astrobiology*, vol. 3, no. 4, pp. 275–285, 2004.
[5] A. Wang, J. J. Freeman, L. Jolliff, and M. Chou, "Sulfates on Mars: A systematic Raman spectroscopic study of hydration states of magnesium sulfates," *Geochimica et Cosmochimica Acta*, vol. 70, no. 24, pp. 6118–6135, 2006.
[6] H. Chen *et al.*, "Raman spectroscopy and X-ray diffraction studies on celestite," *Physica B*, vol. 405, no. 20, pp. 4386–4388, 2010.
[7] L. Frost, A. Wills, L. Weier, and L. Lee, "A Raman spectroscopic study of selected natural jarosites," *Spectrochimica Acta Part A*, vol. 63, no. 1, pp. 1–8, 2006.
[8] N. Buzgar, A. Buzatu, and V. Sanislav, "The Raman study on certain sulfates," *Analele Stiintifice ale Universitatii Al*, vol. 55, no. 1, pp. 5–23, 2009.
[9] J. Brotton and I. Kaiser, "In situ Raman spectroscopic study of gypsum ($CaSO_4 \cdot 2H_2O$) and epsomite ($MgSO_4 \cdot 7H_2O$) dehydration utilizing an ultrasonic levitator," *J. Phys. Chem. Lett.*, vol. 4, no. 4, pp. 669–673, 2013.
[10] K. Ben, H. Kauffmann, H. Aroui, and M. Fontana, "Raman study of cation effect on sulfate vibration modes in solid state and in aqueous solutions," *J. Raman Spectrosc.*, vol. 44, no. 11, pp. 1603–1608, 2013.
[11] M. Harlander, "Spatial heterodyne spectroscopy: Interferometric performance at any wavelength without scanning," Ph.D. dissertation, Univ. Wisconsin–Madison, Madison, WI, USA, 1991, pp. 1–7.
[12] J. Qiu *et al.*, "Broadband transmission Raman measurements using a field-widened spatial heterodyne Raman spectrometer with mosaic grating structure," *Opt. Exp.*, vol. 26, no. 20, pp. 26106–26119, 2018.
[13] J. Qiu *et al.*, "Development of a spatial heterodyne Raman spectrometer with echelle-mirror structure," *Opt. Exp.*, vol. 26, no. 9, pp. 11994–12006, 2018.
[14] J. Qiu *et al.*, "Raman measurements using a field-widened spatial heterodyne Raman spectrometer," *J. Raman Spectrosc.*, pp. 1–12, 2019.
[15] R. Englert and M. Harlander, "Flatfielding in spatial heterodyne spectroscopy," *Appl. Opt.*, vol. 45, no. 19, pp. 4583–4590, 2006.
[16] R. Englert *et al.*, "Correction of phase distortion in spatial heterodyne spectroscopy," *Appl. Opt.*, vol. 43, no. 36, pp. 6680–6687, 2004.
[17] N. Maubec, A. Lahfid, C. Lerouge, G. Wille, and K. Michel, "Characterization of alunite supergroup minerals by Raman spectroscopy," *Spectrochimica Acta Part A*, vol. 96, pp. 925–939, 2012.
[18] D. Fontana, B. Mabrouk, and H. Kauffmann, "Raman spectroscopic sensors for inorganic salts," *Spectroscopic Properties Inorganic Organometallic Compounds*, vol. 44, pp. 40–67, 2013.
[19] H. Zhang and K. Chan, "Understanding the hygroscopic properties of supersaturated droplets of metal and ammonium sulfate solutions using Raman spectroscopy," *J. Phys. Chem. A*, vol. 106, no. 2, pp. 285–292, 2002.
[20] H. Kauffmann, B. Mabrouk, and M. Fontana, "Raman probe for the simultaneous measurement of anion concentration in mixtures of salt solutions," in *Proc. IEEE SENSORS*, 2013, pp. 1–4.
[21] K. Choi and J. Lockwood, "Raman spectrum of Na_2SO_4 (phase V)," *Solid State Commun.*, vol. 72, no. 1, pp. 133–137, 1989.
[22] R. Murugan, A. Ghule, and H. Chang, "Thermo-Raman spectroscopic studies on polymorphism in Na_2SO_4," *J. Phys.: Condens. Matter*, vol. 12, no. 5, pp. 677–700, 2000.
[23] J. Dean and R. Wilkinson, "Precision Raman investigation of the ν_1 mode of vibration of SO_4^{2-}, WO_4^{2-} and MoO_4^{2-} in aqueous solutions of different concentrations," *J. Raman Spectrosc.*, vol. 14, no. 2, pp. 130–134, 1983.
[24] K. Omori, "Infrared diffraction and the far infrared spectra of anhydrous sulfates," *Mineral J.*, vol. 5, no. 5, pp. 334–354, 1968.